Misan Journal of Engineering Sciences ISSN: 2957-4242
Vol. 3, No. 2, Dec 2024 ISSN-E: 2957-4250

Slabless Staircase Flexural Behavior with Multi Reinforcement Configuration

Rafal S. Sabeeh *[1], Prof. Dr. Abdulkhaliq A. Jaafer [2]

[1,2] *Department of Civil Engineering , College of Engineering , University of Misan , Misan, Iraq*
**Corresponding author E-mail: saeedrafal03@gmail.com*

(Received 16 Oct, Revised 13 Dec, Accepted 16 Dec)

Abstract: Slabless staircases represent a modern architectural innovation that eliminates traditional solid stair treads. They employ a series of open or partially supported steps, often reinforced by central support structures or narrow risers. The principal concern with this type of staircase is its flexural strength, which is restricted by the constraints of the steel reinforcement specified in the design criteria. This work investigates the enhancement of RC slabless staircases through the application of unique configurations. The examination of the staircase includes the impact of both standard and high-strength concrete when reinforced with a unique type of steel rebar. Seven models were meticulously developed using the ABAQUS tool and validated against experimental data from the literature. The main characteristics examined were compressive strength and the arrangement of steel reinforcement. The findings indicated a notable enhancement in the ultimate flexural strength of a slabless reinforced concrete staircase utilizing both conventional and high-strength concrete. The reconfiguration of steel bars into a triangular formation in slabless staircases led to a significant enhancement in the final load-bearing capacity, exhibiting varying percentages of improvement: a 25.2% increase in cracking load when compared to traditional models, with ultimate load improvements of 4.8% to 18%, depending on the configuration. The increase of the compressice strength could enhance the ultimate load carrying capacity with ratio reaching to 109%. The deflection increased by 7.8% with altered steel bar configurations, while ductility diminished; however, energy absorption significantly increased by many times as compressive strength rose from 50 to 70 MPa.

Keywords: slabless; flexural strength; steel reinforcement steel fiber; compressive strength

1. Introduction

In order to be able to endure the force of gravity, traditional reinforced concrete (RC) stairs are made with waist slabs that are built beneath the steps during the construction process. However, slab-less reinforced concrete stairs are able to carry the weight solely through the employment of steps and vertical components. This is in contrast to the traditional concrete stairs [1]. A significant similarity may be drawn between this movement and the act of folding plates in half, to put it another way. There are a few other names that can be used to refer to slabless steps. Two of these names are sawtooth staircases and orthopolygonal staircases. In comparison to conventional staircases, the slabless staircase is not a budget-friendly method of construction. This is because of the challenges that are involved with the use of formwork and strengthening. It is still appealing to architects despite this fact since it has a fashionable and visually beautiful aspect [2]. This is the reason why it continues to be popular. The design of slabless stairs is comparable to that of a folded plate, which is the shape of the stairs themselves. The usage of technologies that are not only challenging but also time-consuming is required in order to carry out a full investigation of folded plates. The classic semi-analytical finite strip method and the spline finite strip method are both examples of these technical approaches. In addition, this procedure also makes use of finite strip approaches, which are characterized by the utilization of known shape functions and modified

DOI: https://doi.org/10.61263/mjes.v3i2.116

Fourier series. To facilitate the creation of designs that are more streamlined, scientists have devised a wide range of methodologies and conceptualizations. [3]. Using the techniques of column analogy and second difference, Saenz and Martin [4] came to the conclusion that slabless stairs can be designed using these two methods. Equivalent focused weights were positioned along the axis of the risers in order to replace the scattered gravity force that was previously found. It was considered that the staircase was fastened in an immovable manner at both ends, as indicated by the data contained in the analysis. It was determined from the findings that both approaches yielded the same set of outcomes. Furthermore, the installation also included the reinforcing detailing for a standard staircase that does not have a slab. This was included in the installation. Although the quantity of bending moments that occurred along the length of the staircase varied, the technique in which each step was strengthened was consistent across the whole staircase. To be more specific, the primary bars were arranged in a longitudinal orientation and shaped into stirrups, which are an example of a closed loop. To enhance temperature stability, closed loops were incorporated at the joints, with bars oriented transversely. These transverse bars served a dual purpose which provided structural reinforcement to strengthen the joints, thereby enhancing the overall stability and integrity of the structure, while also facilitating better thermal distribution. The closed-loop configuration of the main bars is believed to enhance the necessary development length and provide resistance against negative moments in the support regions, which may be somewhat constrained. Furthermore, the closed-loop topology can enhance the shear capacity and ductility of the slabs by offering confinement throughout the structure. For the purpose of the research that Benjamin [5] provided, a variety of distinct border settings were taken into consideration. These included staircases with and without landings, among other alternatives. Charts were designed in order to simplify the process of performing computations. Cusens [6] applied the energy (force) technique in order to explore slabless stairs, with the primary emphasis being given on bending moments. This was done in order to analyze the behavior of slabless steps. In order to take into consideration the stress concentration that is likely to be induced by the threaded geometric design of the slabless stairs, it was suggested that the predicted reinforcing area be increased by a factor of two. In spite of the fact that planar straight bars were incorporated into the formation of haunches or fillets at junctions, it was advised that closed loops be utilized for the arrangement of reinforcement. Freestanding slabless staircases were the subject of Solanki's [7] investigation into the examination topic. A landing slab that was of a uniform thickness was also incorporated in these stairs, in addition to an upper and lower flight. As a result of the growth of computers, the finite element method gradually gained popularity, and it started to be utilized in the analysis of slabless stairs a few years ago. On the other hand, the research that was being conducted on this particular staircase has decided to stop. As a result, there are a great deal of limitations that are placed on the investigation that may be carried out in relation to this subject. No one of the papers that were mentioned was supported by research that included a wide range of different variables, according to the researchers' understanding. The experimental and analytical behavior of slabless stairs has only been explored in a very small number of research. The primary reason for this is that concrete possesses a variety of qualities that are quite complicated, including nonlinearity, anisotropy, cracking, and elastoplasticity. Furthermore, the primary means by which behavior is influenced are the particular reinforcement mechanisms that are put into place during the process. Through the utilization of the commercial software ABAQUS, the purpose of this study is to conduct a numerical investigation into the bending properties of slabless stairs. The inquiry will primarily concentrate on alternate reinforcement details and retrofitting treads with multiple configurations of strengthening materials rather than traditional reinforcement features. Despite the fact that the utility of these procedures has not been proved by empirical research, the strength of these steps is based on analytical approaches and technical skills. Because of this, a decision was made to conduct a numerical investigation into the flexural behavior of reinforced concrete staircases that did not contain slabs. This was done in order to determine the consequences of this decision. It is therefore possible to determine whether or not slab-less staircases are feasible, despite the fact that it may be doubtful whether or not they are capable of creating sufficient bending strength while functioning within the authorized deflection limits. Consequently, it is possible to determine whether or not slab-less staircases are feasible. In addition to this, a wide variety of retrofitting techniques were applied in order to improve the flexural strength of RC slabless staircases.

2. Numerıcal Program Fınıte Element Modelıng

The finite element method for nonlinear analysis is widely recognized as a leading technique for simulating concrete structures. During the pre-analysis phase, it is crucial to consider both the material properties and the geometry when modelling beam-column junctions with a finite element (FE) model. It was essential to select the proper components for the materials and replicate the actual behaviour according to the loading and boundary conditions to create a satisfactory model for the experimental test. This was executed as a component of the preprocessing phase. Constitutive models may be considered to simulate the properties of the material. The concrete damage plasticity (CDP) model is utilized to characterize the nonlinear behavior of concrete. Furthermore, the ABAQUS program offers models for brittle cracking and spreading, which are employed for this objective. ABAQUS APDL [8] and computational finite element analysis were employed to conduct a verification method on five slabless staircases to ensure their integrity. The approach employed to verify the previous experimental work conducted by a group of researchers involved utilizing load-displacement relationships, ultimate maximum loads, deflections, and the failure mechanism. [8-10].

3. Finite Element Discretization

It is well acknowledged that employing the finite element method for nonlinear analysis is one of the most advanced techniques for simulating concrete structures. During the pre-analysis phase, it is crucial to consider both the material properties and the geometry when modelling beam-column junctions with a finite element (FE) model. It was essential to select the proper components for the materials and replicate the actual behaviour according to the loading and boundary conditions to create a satisfactory model for the experimental test. This was executed as a component of the preprocessing phase. Constitutive models may be considered to simulate the properties of the material. The concrete damage plasticity (CDP) model is utilised to characterise the nonlinear behaviour of concrete. Furthermore, the ABAQUS program offers models for brittle cracking and spreading, which are employed for this objective. ABAQUS APDL and computational finite element analysis were employed to conduct a verification procedure on five slabless staircases to ensure their structural integrity. The approach employed to verify the previous experimental work conducted by a group of researchers involved utilising load-displacement relationships, ultimate maximum loads, deflections, and the failure mechanism [8-10].

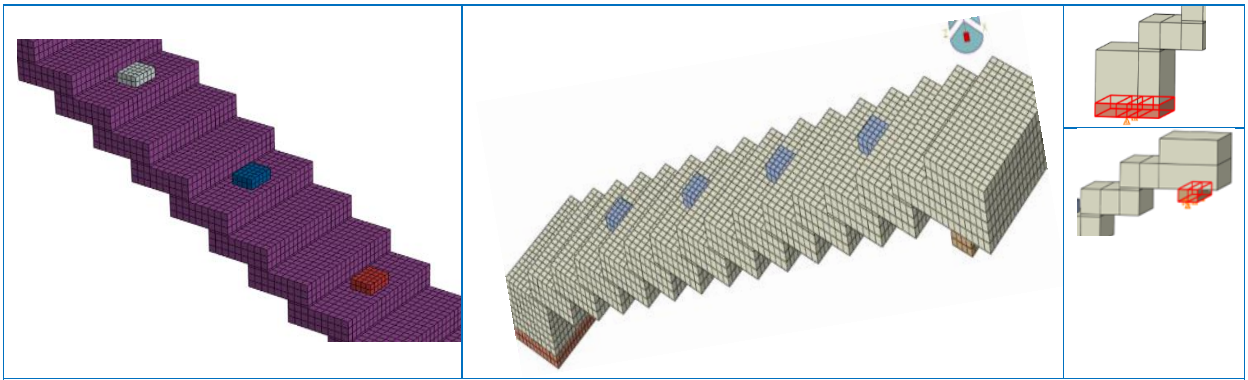

Fig. 1. The finite element model shows the modeling stairs component.

Furthermore, it was discovered that there was a significant amount of matching in the number of elements that exceeded 15000 elements with element sizes don’t exceeds 50 mm. The improved mesh and input values were subjected to convergence circumstances, which led to the discovery of this. A representation of the modeling and meshing of the specimens that were studied may be found in Figure 1. [15, 16]

4.Material Modeling Concrete and Steel Reinforcement

Modelling concrete in ABAQUS necessitates the delineation of its material properties, characterized by quasi-brittle behavior and exhibiting distinct attributes in compression compared to tension. Approximately 30 % of the concrete's compressive strength (f_{cu}) demonstrates linear behavior in the stress-strain curve, known as the elastic stage, on the compression side of the material. As the yield point is reached, tension will gradually increase until it achieves its maximum level. Once maximum strain is attained, the curve starts to descend into the softening region, hindering the attainment of ultimate compressive strength. [11]. The tension behavior exhibited a linear growth of the curve until it attained the maximum tensile strength, which various studies estimate to be between eight and twelve percent of the compressive strength. Upon reaching its yield point, concrete commences fracturing and gradually loses strength until it ultimately breaks, culminating in its crushing, as depicted in Fig. 2. The ultimate uniaxial compressive strength, ultimate uniaxial tensile strength, elastic modulus (E), modulus of rupture, Poisson's ratio, and stiffness reduction factor are parameters employed to evaluate concrete performance in ABAQUS [18]. It should be noted that the properties of the concrete and steel defined into the model through the input material properties. The behavior of standard concrete under uniaxial compression can be explained by the constitutive model of standard concrete [11]. Plasticity is utilised to evaluate damage indicative of concrete behavior. The fundamental elements of a staircase in ABAQUS consist of concrete and steel reinforcement, integrated into the concrete framework. To accurately imitate the behavior of slabless stairs under flexural stresses, it is crucial to emulate the characteristics of the actual materials employed in the components. The ABAQUS program offers a comprehensive range of geometric relationships for modelling various elements, facilitating the creation of models from several components. Numerical integration is utilized in all aspects of the model to ensure accurate material performance. Moreover, the attributes of elements can be defined as generic sections, with numerical integration executed for each cross-section of the component. This indicates that all elements are quantitatively integrated.

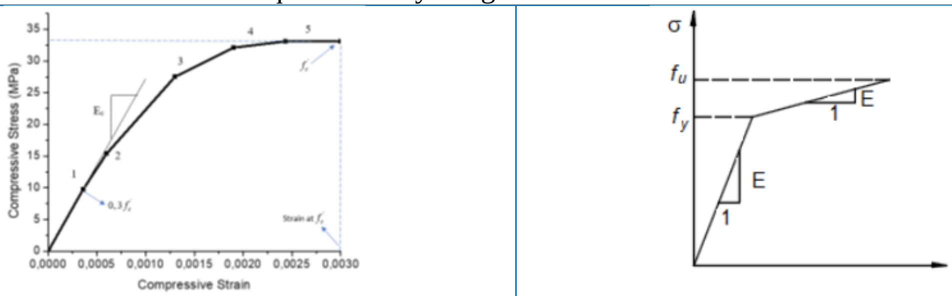

(a) (b)

Fig. 2. Stress-strain relationship for steel and concrete [11]
Stress-strain curve for concrete under compression (b) Stress-strain curve for steel reinforcement.

The Concrete Damage Plasticity (CDP) model, provided by the ABAQUS library, was employed in the present model. The model incorporates the notion of isotropic damaged elasticity alongside compressive plasticity or isotropic tensile behavior. The model distinguishes irreversible concrete damage from fracture through the incorporation of scalar damaged elasticity and non-associated multi-hardening plasticity. The model posits that the two primary failure modes of concrete are tensile cracking and compressive crushing. The enlargement of failure surfaces is regulated by two hardening variables that define the failure process during material compression or tension. [13]. The characteristics of the damaged plasticity model are defined by the degradation that occurs under tensile and compressive stresses. The element's elastic stiffness diminishes due to impaired characteristics, making the original elastic stiffness irrecoverable. Static loading is a critical concern, as the tensile and compressive components of the damage contribute to overall degradation. [14]. Concrete was modelled using C3D8R with a multilinear stress-strain curve for material representation. T3D3 with an elastic linear stress-strain relationship was utilized to model the steel reinforcement bar as specified in Table 1.

Table 1. Properties of materials [17].

Concrete Type	*f'c* [MPa]	E (GPa)	Tensile Strength [MPa]	Thickness	Adopted Stress-Strain Curve
Concrete	20-50	Variable	Variable	-	Multilinear stress-strain curve
Steel reinforcement	-	200	400	-	Bilinear stress-strain curve

5.Verification of Finite Element Model

For the purpose of verifying the proposed finite element model, the experimental data that was published by Özbek et al. [17] was utilized. In terms of size, material features, and boundary conditions, the model that was utilized in this investigation is identical to the one that was used there [17]. The verification led to the discovery that there was an exceptionally high level of concordance between the findings gained from the experiments and the numerical calculations about the load deflection, test outcomes, and cracking pattern. This is seen in Figure 3, which shows the results of the verification. In spite of the fact that the agreement of validation was quite high, it is essential to point out that certain curves of the numerical analysis reached the maximum load and then ceased. The reason for this was that the concrete element that was utilized in the analysis had a characteristic in which the failure of any component of the model was considered to be a failure of the entire member. This was the reason why this consequence occurred. A reasonable concordance in terms of load and mid-span deflection is demonstrated by the data that are produced by the numerical model. However, ABAQUS models display a greater degree of stiffness in the elastic zone of the load-deflection curve. This is in contrast to another type of model. This becomes more apparent when looking at the figures for the T and C groups (the C, t, and T series refers to the configuration of the steel reinforcement in the validated study [17]. On the basis of the comparison between the ABAQUS model and the experimental specimens, a detailed analysis is shown in Table 2 and Figure 3, respectively. It is vital to carefully analyze the inherent discretization mistakes that occur in finite element analysis in order to conduct a comprehensive study of the quantitative results that were produced from examining the suggested ABAQUS model. As a result of the findings of the comparative research that are presented in this article, the ABAQUS model that was provided for the prototype examination is considered to be reliable and accurate. This conclusion is arrived at by taking into account the variables that were stated earlier. In the case of the mismatch agreement values, particularly for physical models, these inaccuracies are the result of translating a mathematical model into a finite-element one, which is characterized by a finite number of degrees of freedom. The solution arrived at using finite element analysis is influenced by a number of factors, including the number of elements, the number of nodes that are associated with each element, the shape functions of elements, the integration rules, and the formulation details of particular elements. On the basis of the comparison between the ABAQUS model and the experimental specimens, a detailed analysis is shown in Table 2 and Figure 3, respectively. It is vital to carefully analyze the inherent discretization mistakes that occur in finite element analysis in order to conduct a comprehensive study of the quantitative results that were produced from examining the suggested ABAQUS model. As a result of the findings of the comparative research that are presented in this article, the ABAQUS model that was provided for the prototype examination is considered to be reliable and accurate. This conclusion is arrived at by taking into account the variables that were stated earlier. In the case of the mismatch agreement values, particularly for physical models, these inaccuracies are the result of translating a mathematical model into a finite-element one, which is characterized by a finite number of degrees of freedom. The solution arrived at using finite element analysis is influenced by a number of factors, including the number of elements, the number of nodes that are associated with each element, the shape functions of elements, the integration rules, and the formulation details of particular elements.

Table 2. The results of the validated comparison between the numerical study and the experimental study.

	Experimental				Abaqus				$V_{ABAQUS}/V_{Exp.}$			
	Uy	**Py**	**Uf**	**Pf**	**Uy**	**Py**	**Uf**	**Pf**	**Uy**	**Py**	**Uf**	**Pf**
t100/100	52	22	121	21.3	51.58	21.8	130.7	25.166	1	1	-8	-18
t100/80	53.9	22.47	120	20.3	62	23	125	24	-15	-2	-4	-18
t80/100	61	16	120	18	68	18	131.7	22	-11	-13	-10	-22
T100/100	62.8	31	144.7	32	52.77	34.8	148.32	38.6116	16	-12	-3	-21
T100/80	65.4	27.9	127.3	32.6	51.5	31.6	138.1	34.72	21	-13	-8	-7
T80/100	69	25	142	26.6	48	23	155	30	30	8	-9	-13
C100/100	69	29	111.65	34	49.47	32.5	126.67	36.6	28	-12	-13	-8
C100/80	64.4	30	120	33	53	33	129	37	18	-10	-8	-12
C80/100	64.2	23.5	111	28.2	47.7	23.8	126.6	31	26	-1	-14	-10

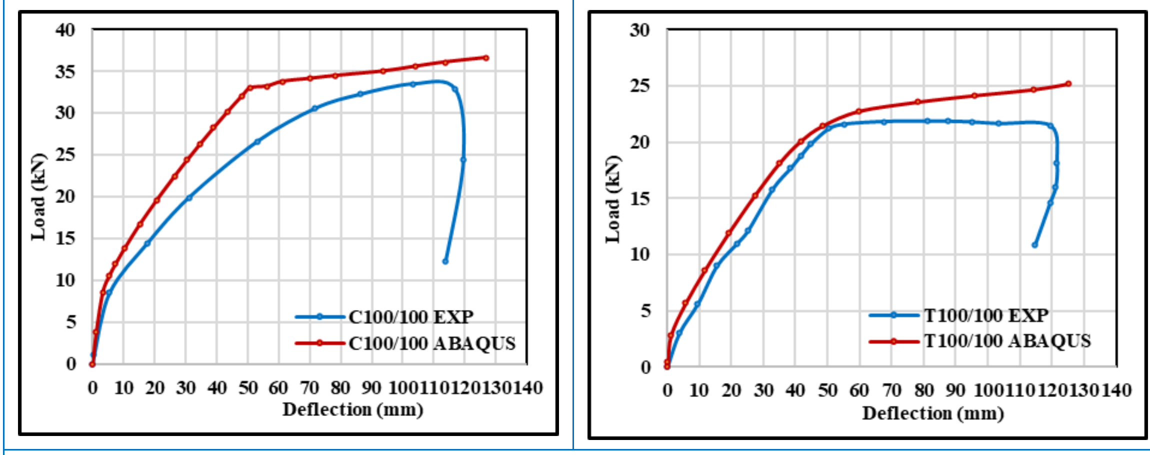

Fig. 3. Load-deflection curve of experimental vs. numerical data.

6.Specimens Detail

To enhance the parametric analysis required for the slabless staircase response, the validated finite element model was employed. This study entailed the design and analysis of nine staircases constructed from reinforced concrete. Standard dimensions are generally employed in practical applications. Fourteen steps were positioned on the staircase, situated between two beams. Each beam included a cross section measuring 200 millimetres by 300 millimeters, consistent at both ends. The subsequent list delineates the measurements of the steps, derived from the information depicted in Figure 4: The stair width (bw) is 600 millimeters, the tread width (t) is 200 millimeters, and the riser height (r) is 110 millimeters. The tread thickness (th) and riser thickness (tv) of slabless stairs can be designed to be either identical or distinct, as they are not components of a unified structure. Considering the anticipated effects on both strength and behavior, the test parameters of th and tv were evaluated and analyzed due to their influence. When the thicknesses are large, however, this inquisitiveness is diminished. Consequently, it was decided that the thicknesses that are going to be investigated are either 100 millimeters or 100 millimetres wide. The slabless stairs were modelled as part of the parametric study, which also included the introduction of several properties such as the specimens' compressive strength and steel arrangement. Many distinct values for the compressive strength of concrete were contained within the range of that variable. This group contained values between 50 and 70 MPa. The staircases were fortified with steel bars arranged in a triangle pattern, with each tread beginning, middle, and ending with a triangle. The strut and tie method were the foundation of this steel reinforcement configuration method, as seen in Figure 4.

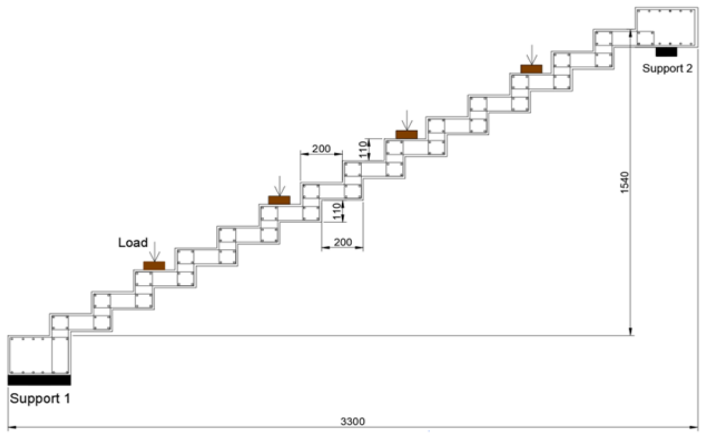

(a)

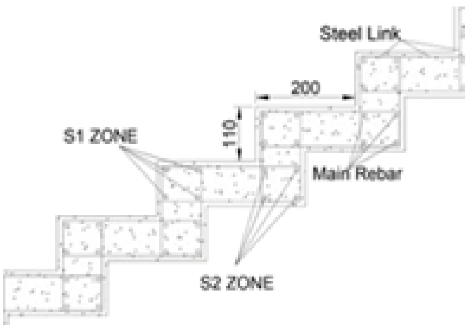

(b)

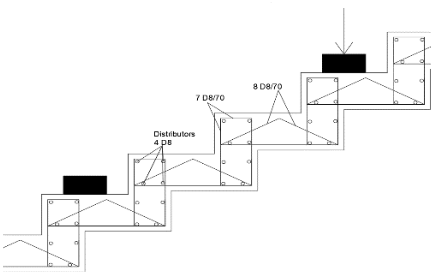

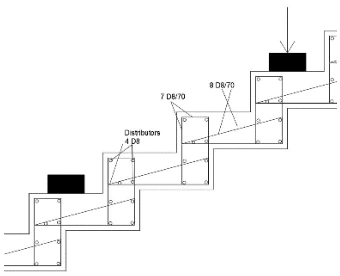

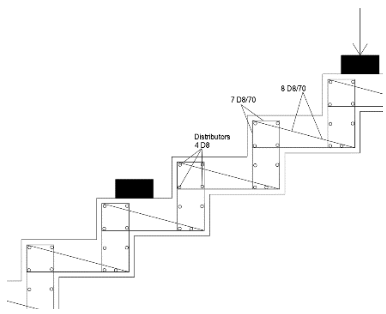

(c) (d) (e)

Fig. 4. Demonstrations of geometry tests
(a) Slabless Staircases Model (ST) (b) S-Zones distribution (c) ST-M (d) ST-L (e) ST-R.

Table 3. Description of Specimens.

Var.	Beam	*f'c (MPa)*	Variable Details
Steel bars configuration	ST	50	-
	ST-M	50	Configuring the steel bars in triangular form from the right
	ST-L	50	Configuring the steel bars in triangular form from the left
	ST-R	50	Configuring the steel bars in triangular form from the right and left
Compressive Strength	ST-M -70	70	Change the compressive strength to 70 MPa
	ST-L-70	70	Change the compressive strength to 70 MPa
	ST-R-70	70	Change the compressive strength to 70 MPa

7.Results and Discussion

Specifically, Table 4 shows and summarizes the specimen data for cracking load, ultimate load, load-deflection curves, stiffness, energy absorption, and failure mode, as well as for ductility index and ultimate load.

Table 4. Test result of Load Deflection Curve.

ID	Cracking Load kN	Deflection mm	Ultimate Load kN	Deflection mm	Initial Stiffness kN/mm	Ductility Index	Energy Absorption (kN.mm)
ST	10.48	28.68	38.61	148.33	1.10	5.17	281.65
ST-M	13.12	30.93	40.47	161.84	1.27	5.12	467.50
ST-L	11.64	51.12	41.36	174.24	0.68	3.41	639.15
ST-R	13.54	48.52	45.56	165.37	0.84	3.41	681.80
ST-M -70	16.59	25.12	63.26	111.18	1.98	4.43	1230.44
ST-L-70	15.03	34.61	69.19	100.71	1.30	2.91	749.95
ST-R-70	18.75	35.08	80.90	104.68	1.60	2.98	1105.50

7.1 Effect of Bar Configuration

Partially replacing the steel reinforcement with the new configuration bars based on the strut and tie analysis helped alleviate the effects of steel rebar on the flexural behaviour of slabless staircases. Specifically, the steel bars were installed at S1, S2, and the S1-S2 zones to replace the steel reinforcement. The behavior was better in comparison to the traditional models when the steel reinforcement configuration specimens were modified. A cracking load of 10.48 kN is displayed by the model (ST). But when the steel reinforcement was rearranged into a triangle with the head positioned in the middle of the tread span, the cracking load rose to 11.12 kN, a 25.2% increase from the model (ST). It was also determined that the cracking resistance increased less when the steel reinforcing bar in the S1 zone (ST-L) was replaced compared to the S1-S2 zone (ST-M). The reason behind this is that one area experiences more stress compared to another. Figure 5 shows that placing the triangle shape of the steel bars in the starting zone (S1 zone) increased the cracking load by 11.1%, whereas placing the same shape at the end of the treads in the S2 zone increased the cracking load by 29.2%. The ultimate load, as shown by the model (ST), is 38.61 kN. The ultimate load (model ST-M) increased to 40.47 kN, or 4.8% more than the model (ST), when the steel reinforcement was rearranged to a triangle shape with the head positioned in the middle of the tread span. It was also determined that the ultimate resistance increased less when the steel reinforcing bar in the S1 zone (ST-L) was replaced compared to the S1-S2 zone (ST-M). Figure 6 illustrates that positioning the triangular configuration of steel bars in the starting zone (S1) resulted in a 7.1% increase in ultimate load, whereas mirroring the triangular configuration to the S2 zone (at the end of the treads) yielded a greater increase of 18% in ultimate load. The model (ST) demonstrates a deflection of 9.56 mm. Upon altering the configuration of the steel reinforcement to a triangle shape with the apex positioned at the mid-span of the tread which the apex led to more distribution of stresses with less resistance to deflection, the deflection (model ST-M) escalated to 10.31 mm, representing a 7.8% increase relative to the model (ST). Furthermore, it was determined that substituting the steel reinforcing bar in the S1 zone (ST-L) led to a deflection increase that was inferior to that observed in the S1-S2 zone (ST-M). This is because this region experiences greater stressors than another region. Figure 5 illustrates that positioning the triangular configuration of steel bars in the starting zone (S1) resulted in a deflection increase of 78.2%, whereas mirroring the triangular configuration to the S2 zone (at the end of the treads) led to a deflection increase of 69.2%.

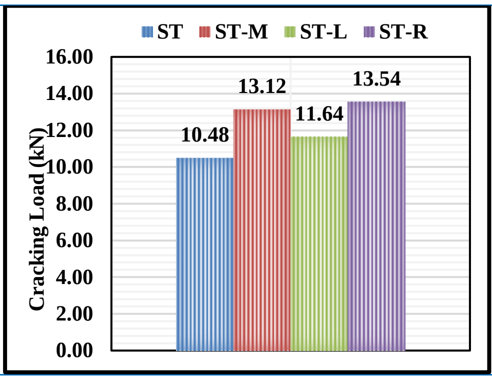

(a)

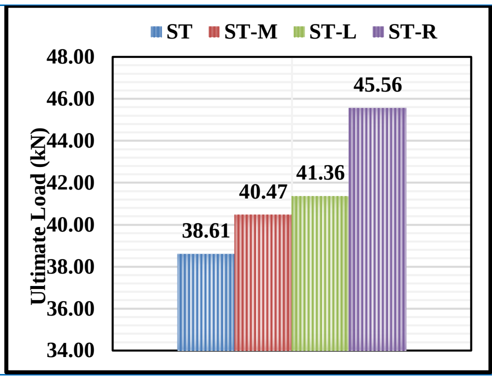

(b)

Fig. 5. Cracking and ultimate load results
(a) Cracking load of ST-series (b) Ultimate load of ST-series.

7.2 Effect of Compressive Strength

The results of the testing of RC staircases that were subjected to flexural stresses are detailed in Table 4 and Figs. 5 and 6. Substantial variations were identified among the concrete slabless stairs. The difference was attributed to the substantial impact of concrete strength on the staircase response. In order to examine the impact of the compressive strength of concrete on the flexural behaviour of staircases, the compressive strength values were altered between 50 and 70 MPa. The specimen (ST-M-70) exhibited a higher cracking load resistance of 16.59 kN when contrasted with the corresponding model of conventional concrete (ST-M). The compressive strength of the concrete was directly proportional to the fracture load. According to Fig. 6, the fracture strength of models (ST-M-70, ST-L-70, and ST-R-70) increased by approximately 58.3%, 43.4%, and 78.9%, respectively, as the compressive strength increased from 50 to 70 MPa. The maximum load values in Fig. 6 were significantly improved by approximately 63.8%, 79.2%, and 109.5%, respectively, as a result of the increase in concrete compressive strength from 50 to 70 MPa. The deflection behaviour was dissimilar to that of fracture and ultimate load, as the deflection decreased as the compressive strength increased, as illustrated in Fig. 6.

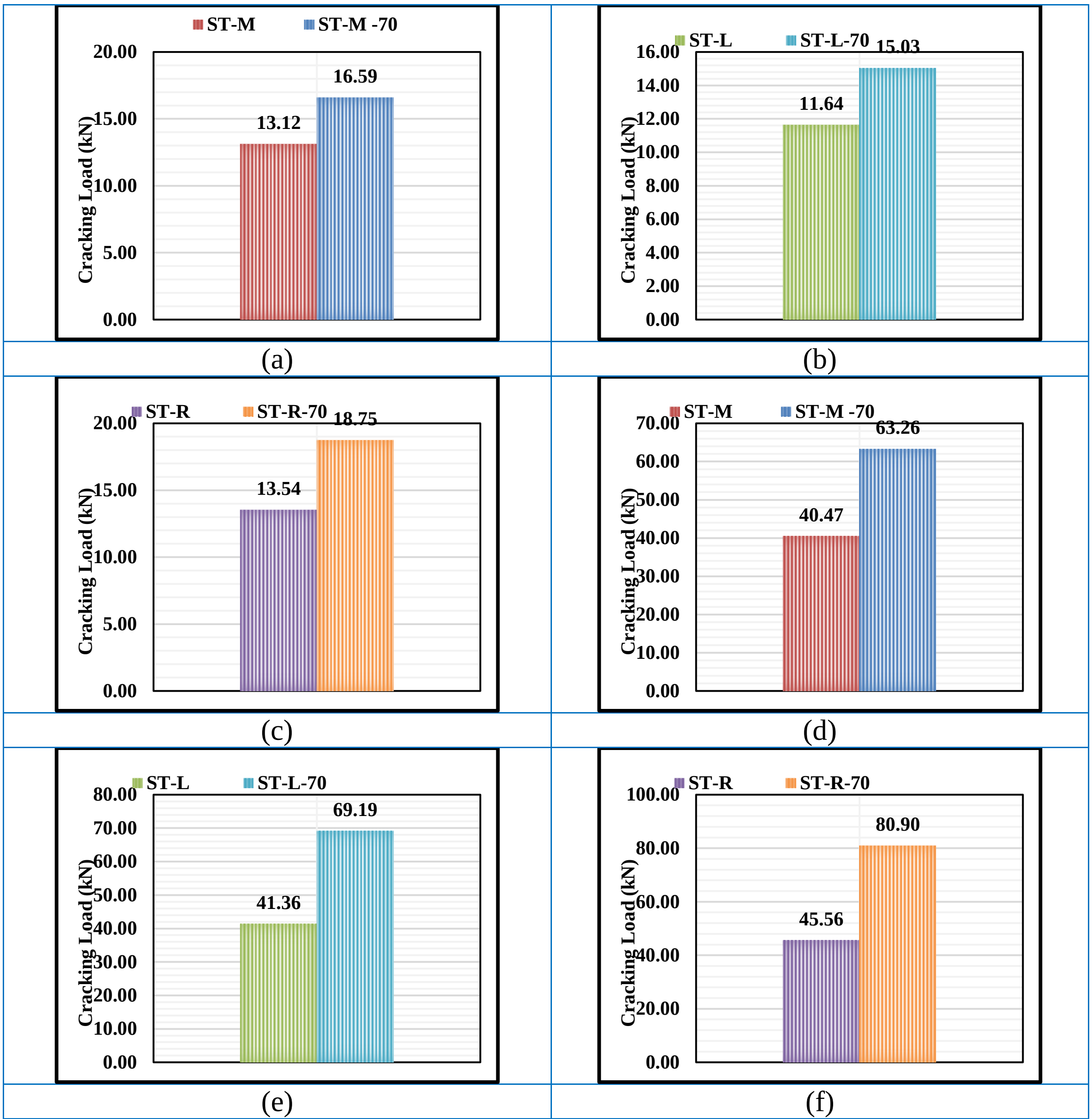

Fig. 6. Cracking and ultimate load results.
(a) Cracking load of ST-M (b) Cracking load of ST-L (c) Cracking load of ST-R
(d) Ultimate load of ST-M (e) Ultimate load of ST-L (f) Ultimate load of ST-R.

7.3 Ductility Index

The material's ability to endure substantial deformation without experiencing abrupt failure is denoted by the term "ductility index" [18]. Constructions composed of ductile concrete may exhibit visible deformations, including cracking and bending, when subjected to static stresses. Internal reinforcement is one of the factors that can alter the ductility of concrete, as it can considerably enhance the material's ductility. This contributes to the management and distribution of cracking, as well as the reduction of abrupt failure and the provision of additional strength. By computing the ratio of the ultimate deflection (Δu) to the yield deflection (Δy), the ductility can be determined [18]. The material's ductility is determined by this ratio. Slabless staircases' ductility index results are illustrated in Table 4 and Fig. 7, respectively. The specimen with the highest ductility index was the ST, which measured 5.17. The ductility decreased to 5.12 when the steel reinforcement was reconfigured in a triangular shape with the head located in the mid-span of the tread, which is equivalent to a 1% decrease in comparison to the ST model. This is in reference to the impact of the steel configuration. In addition, it was determined that the ductility was diminished as a consequence of replacing the steel reinforcing bar in the S1 zone (ST-L). The reason for this is that this region is subjected to greater stresses than another region. Fig. 6 illustrates that the ductility decreased by 34% when the triangular steel bars were inserted into the start zone (S1 zone). Conversely, the ductility decreased by 34.1% when the steel triangular configuration was mirrored in the S2 zone (at the end of the treads). As the compressive strength of the concrete increased, the ductility index decreased. For models with compressive strengths of 70 MPa, the ductility index decreased by 14.4%, 44%, and 42.3%, respectively, as the compressive strength of the material was increased from 50 to 70 MPa.

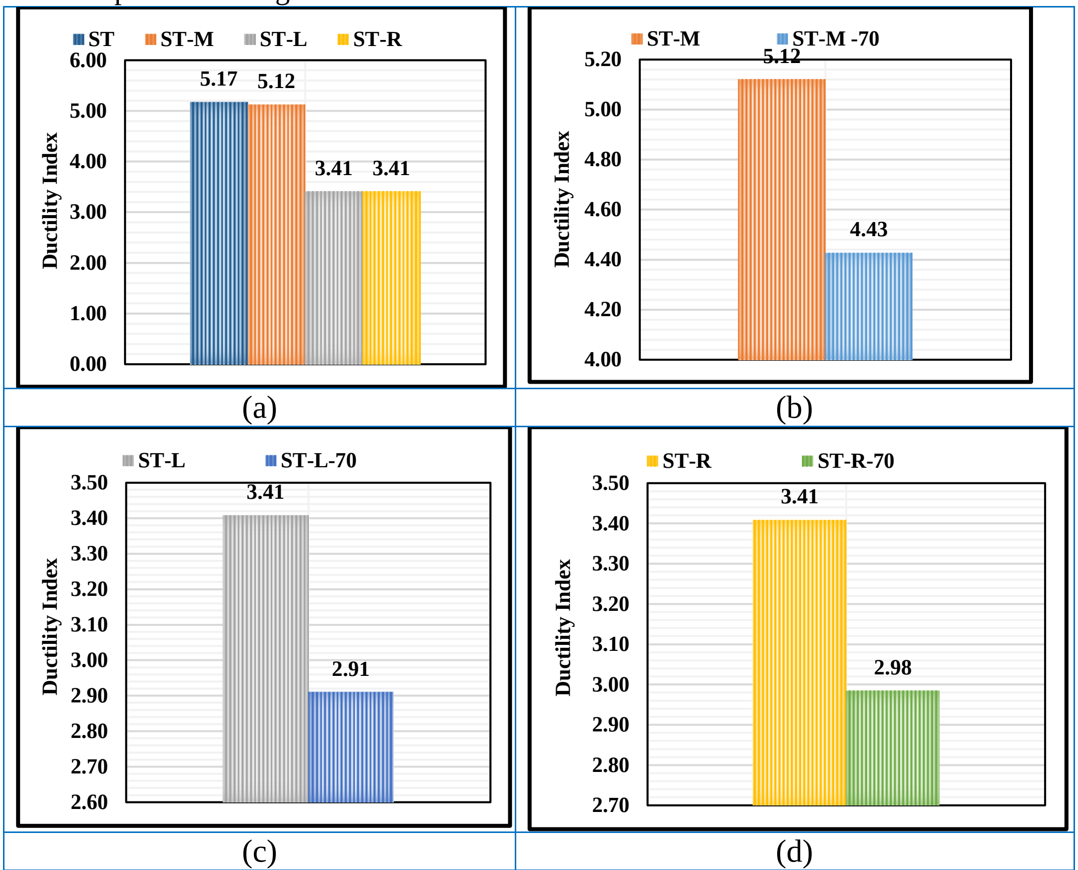

Fig. 7. Ductility index of the slabless staircases.

7.4 Energy Absorption

Calculating the integral of the load deflection curve is a method that may be utilised to quantify the amount of energy that is absorbed. It is the gradient of the starting portion of the load-deflection curve that is referred to as the initial stiffness that is being discussed. In order to perform the computation, it is necessary to divide the yield load (Py) by the yield deflection (Δy). The data on the energy absorption of slabless staircases are presented in Table 5 and Figure 8, respectively. An energy absorption of 281.65 kN.mm was discovered to be the highest among the specimens, and the ST was revealed to be the representative of this. When the configuration of the steel reinforcement was altered to a triangle form with the head resting in the middle span of the tread, the energy absorption increased to 467.5 kN.mm, which is comparable to 66% when compared with the model (ST). This was in reference to the effect that the steel configuration had. The replacement of the steel reinforcing bar in the S1 zone (ST-L) was shown to result in an increase in the amount of energy that was absorbed, as was another conclusion reached. As shown in Figure 6, it is demonstrated that the triangular configuration of steel bars in the start zone (S1 zone) resulted in an increase in the energy absorption with a percentage of 126.9%. On the other hand, when the steel triangular configuration was mirrored to the S2 zone (at the end of the treads), the energy absorption increased with a percentage of 142%. When the compressive strength of the concrete increases, there is a large rise in the amount of energy that is absorbed by the concrete. It was found that the energy absorption of the material rose by 616%, 336.8%, and 292.5% respectively for models (with compressive strengths of 70 MPa) when the compressive strength of the material was increased from 50 to 70 MPa.

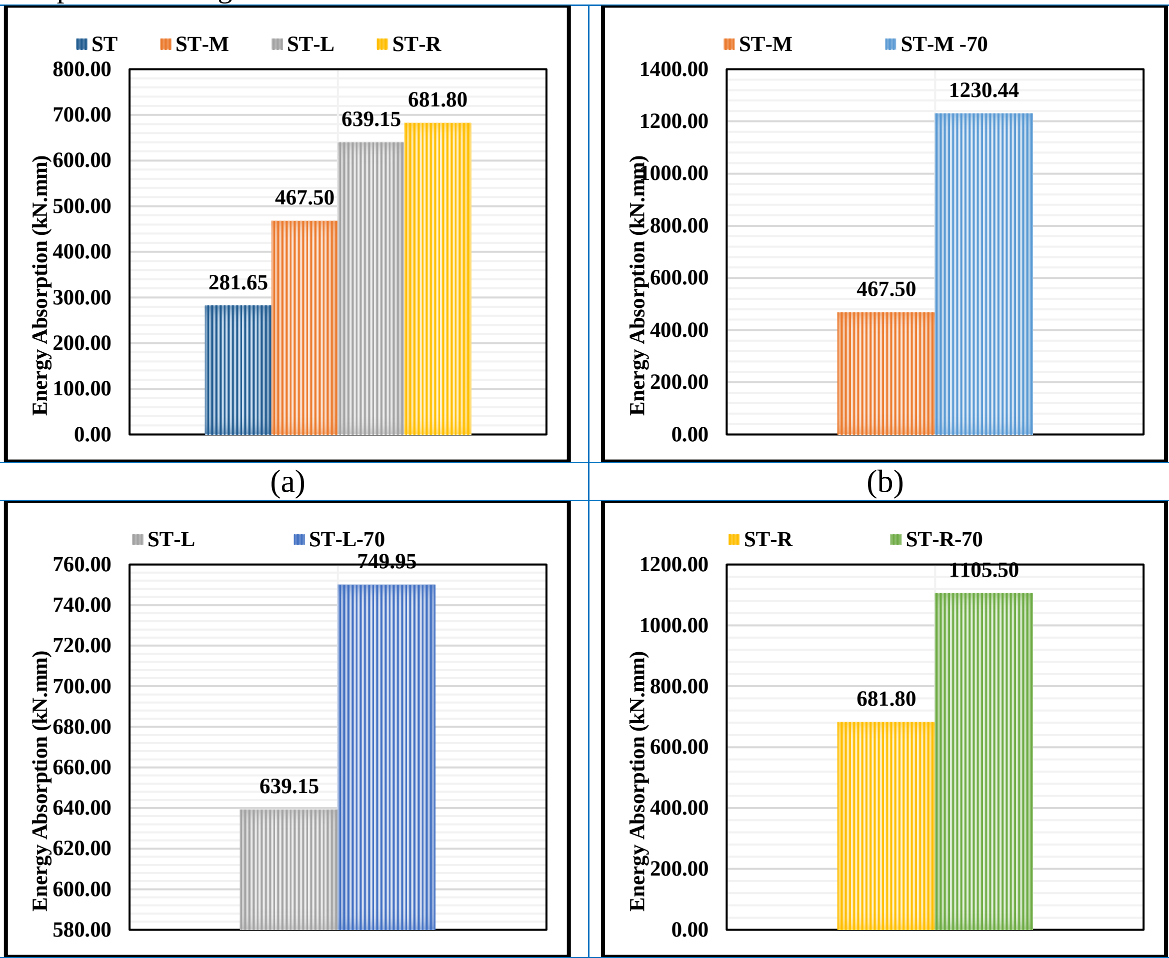

(a) (b) (c) (d)

Fig. 8. Energy Absorption of the slabless staircases

7.5 Cracking and Failure Mode

In models (ST-M-70) to (ST-R-70), which included simulating slabless stairs with varied compressive strengths, it was demonstrated in Figure 10 that the distribution of stresses did not change as the compressive strength increased. This was the case in all of the models included in the study. In the process of implementing a new configuration of steel reinforcement, the stress distribution was influenced by the utilisation of steel rebar. The results showed that the stresses were concentrated most intensely in the S1 zones when steel rebar was replaced with triangular rebar. Other areas of the structure had lower concentrations of stresses than the S1 zones. Following the replacement of the steel rebar in the S2 zone, the concentration was found to be higher in comparison to the experimental model.

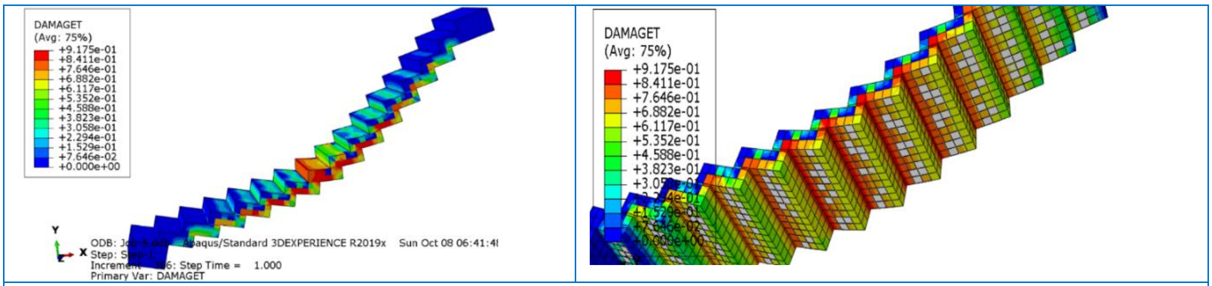

(a) ST

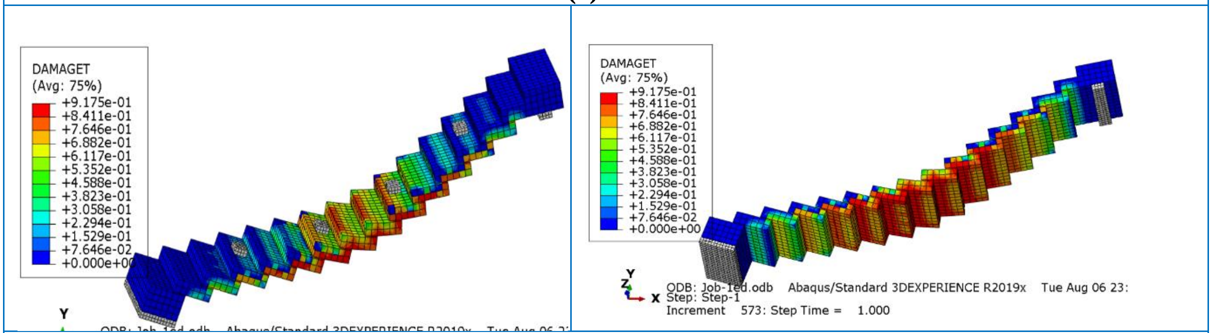

(b) ST-M

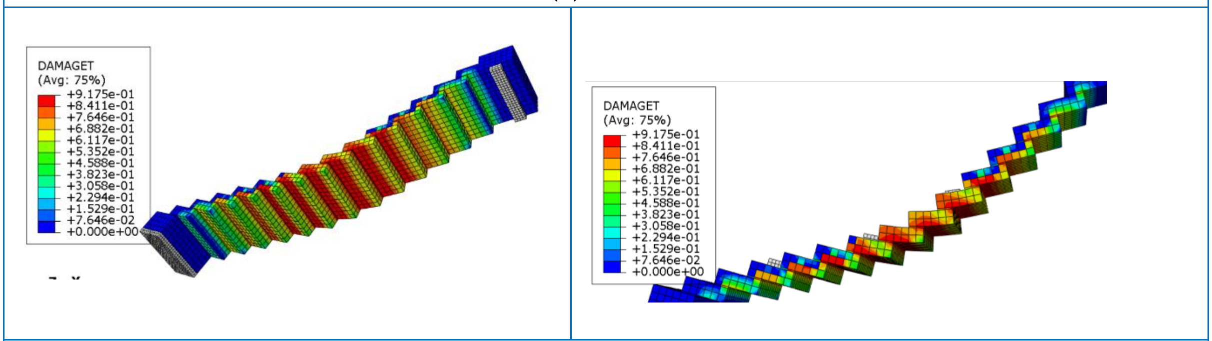

(c) ST-L

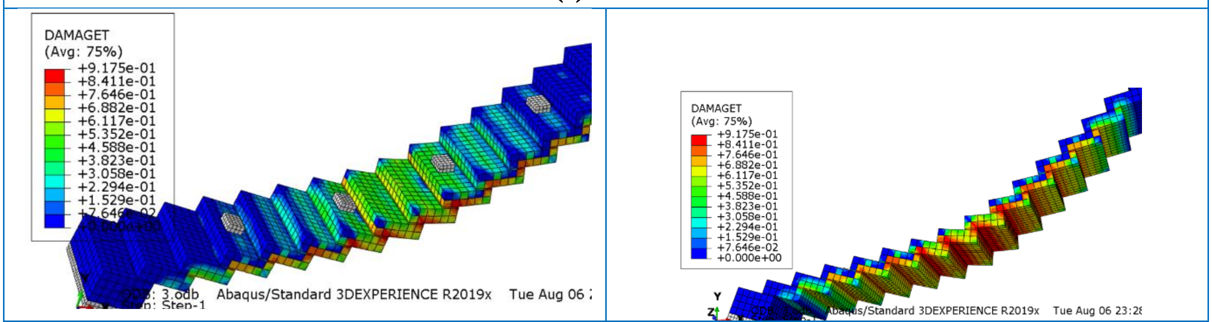

(d) ST-R

Fig. 9. Cracks pattern for slabless staircases.

8. Conclusions

The purpose of this study was to explore the flexural behavior of concrete staircases that did not contain slabs and were strengthened using all kinds of different techniques. The ensuing deductions are able to be made on the basis of the findings that were obtained.:

1-Rearrangement of the steel reinforcement in the strut and tie method enhanced the structural behavior of slabless staircases.

2-The slabless staircases flexural strength developed a substantial increase in the ultimate load carrying capacity when the steel configuration changed from conventional to new configuration method.

3-The triangular configuration of steel bars, particularly when placed at the mid-span of the tread, resulted

in the highest observed cracking load, indicating that strategic placement of reinforcement can optimize structural performance.
4-Increasing the compressive strength of the concrete from 50 to 70 MPa led to significant improvements in both cracking load resistance and ultimate load capacity, highlighting the importance of material properties in staircase design.
5-Although the reconfiguration of steel reinforcement resulted in increased loads, it also slightly decreased the ductility index. This underscores the need for a balance between strength and ductility in design to avoid sudden failure.
6-The research revealed that energy absorption capabilities improved markedly with the triangular reinforcement configuration, suggesting that this design may enhance the overall resilience of slabless staircases under load.
7-The study found that the concentration of stresses varied significantly based on the configuration of steel reinforcement, which has implications for future design considerations and the placement of reinforcement in critical zones.
8-The results indicated that the performance of triangular steel bars was superior in terms of load-bearing capacity compared to conventional configurations, emphasizing the potential benefits of innovative reinforcement methods.
9-These findings advocate for the consideration of alternative reinforcement configurations and higher concrete compressive strengths in the design of slabless staircases to enhance their structural integrity and performance under load.

Author Contributions: The authors contributed to all parts of the current study.
Funding: This study received no external funding.
Conflicts of Interest: The authors declare no conflict of interest.

References

[1] S. Yingjie, Y. Gong, Y. Wang, Q. Zhou, X. Li, F. Ding and Y. Kuang. "Flexural behavior of ultra-high performance concrete (UHPC) shaped thin-plate ribbed staircases: an experimental and numerical study," Mater. Struct. 57, 1 (2024).
[2] R. J. Jiang and F. T. K. Au, "A General Finite Strip for the Static and Dynamic Analyses of Folded Plates," Thin-Walled Struct. 49, 1288–1294 (2011).
[3] Q. W. Su, "Finite Element Analysis of Staircase under Earthquake Action," Adv. Mater. Res. 2964–2968 (2010).
[4] L. P. Saenz and I. Martin, "Slabless Tread-Riser Stairs," ACI J. Proc. 58, 353–366 (1961).
[5] B. S. Benjamin, "The Analysis of Slabless Tread-Riser Stairs," Indian Concr. J. 36, 443–447 (1962).
[6] A. R. Cusens, "Analysis of Slab-Less Stairs," Concr. Constr. Eng. 61, 359–364 (1966).
[7] H. T. Solanki, "Freestanding Stairs with Slabless Tread-Risers," J. Struct. Div. ASCE 101, 1733–1738 (1975). https://doi.org/10.1061/JSDEAG.0004150.
[8] S. Sharma, "Finite Element Analysis of Slabless Tread Riser Stairs," Master's thesis, Department of Civil Engineering, University of Roorkee, Roorkee, India, 1993, 120 pp.
[9] T. Tejaswini and Dr. M.V.Rama Raju, "Analysis of RCC Beams using ABAQUS," Int. J. Innov. Eng. Technol. 5 (2015).
[10] D. T. Hashim, A. W. Abdulghani, and H. M. A. Albegmprli, "Case study of shear strengthening of RC Corbels by steel plates using fea," East.-Eur. J. Enterp. Technol. 2(7 (122), 50–60 (2023).
[11] D. Kachlakev, T. Miller, S. Yim, K. Chansawat, and T. Potisuk, American Society for Testing and Materials. Report SPR 316 (California Polytechnic State University, San Luis. Obispo, CA and Oregon State University, Corvallis OR for Oregon Department of Transportation, 2001).
[12] J. Lubliner, R. L. Taylor, and F. Auricchio, "A new model of generalized plasticity and its numerical implementation," Int. J. Solids Struct. 30, 3171–3184 (1993).
[13] G. Abaqus, "Abaqus 6.11," Dassault Systemes Simulia Corporation, Providence, RI, USA, 2011, p. 3.
[14] ASCE 7-16, "Minimum Design Loads and Associated Criteria for Buildings and Other Structures," American Society of Civil Engineers, Reston, VA, 2017, 800 pp.

[15] A. W. Abdulghani and A. Jaafer, "Comparative Numerical Study between/Steel Fiber Reinforced Concrete and SIFCON on Beam-Column Joint Behavior," Mater. Sci. Forum 1021, 138–149 (2021).
[16] A. A. Jaafer and A. W. Abdulghani, "Nonlinear finite element analysis for reinforced concrete haunched beams with opening," IOP Conf. Ser.: Mater. Sci. Eng. 454, 012152 (2018).
[17] L. Wang, J. Yi, J. Zhang, W. Chen, and F. Fu, "Short-term flexural stiffness prediction of CFRP bars reinforced coral concrete beams," Materials 14, 467 (2021).
[18] E. Özbek, Y. Kaya, M. Bocek, and S. Aykaç, "Flexural Behavior of Slabless Reinforced Concrete Staircases," ACI Struct. J. 118 (2021).
[19] M. J. N. Priestley and R. Park, "Strength and ductility of concrete bridge columns under seismic loading," Struct. J. 84, 61–76 (1987).
[20] T. J. Sullivan, G. M. Calvi, and M. J. N. Priestley, "Initial stiffness versus secant stiffness in displacement based design," 13th World Conf. Earthq. Eng. (WCEE) 65, 2888 (2004).